Available online at www.sciencedirect.com
ScienceDirect
Remote Sensing of Environment 105 (2006) 354–366
Remote Sensing of Environment
www.elsevier.com/locate/rse

Estimating vegetation water content with hyperspectral data for different canopy scenarios: Relationships between AVIRIS and MODIS indexes

Yen-Ben Cheng [a,*], Pablo J. Zarco-Tejada [a], David Riaño [a,b], Carlos A. Rueda [a], Susan L. Ustin [a]

[a] *Center for Spatial Technologies and Remote Sensing (CSTARS), Department of Land, Air, and Water Resources (LAWR), One Shields Avenue, The Barn, University of California, Davis, CA 95616, USA*

[b] *Departamento de Geografía, Universidad de Alcalá, Colegios 2, E-28801 Alcalá de Henares, Madrid, Spain*

Received 17 April 2006; received in revised form 6 July 2006; accepted 15 July 2006

Abstract

Three linked leaf and canopy radiative transfer models were used to assess uncertainties in three vegetation architectures for the relationships between canopy water content and Equivalent Water Thickness (EWT). The leaf radiative transfer model PROSPECT was linked to SAILH, rowMCRM, and FLIM canopy reflectance models to generate synthetic spectra for a range of leaf and canopy parameters under closed, row-structured, and forest canopy architectures, respectively. Leaf water content (C_w) and leaf area index (LAI) were used to calculate canopy water content. Leaf and canopy parameters that affect the retrieval of EWT, estimated by the MODTRAN-based fitting technique, were used to investigate their influence on the water content estimates. Results showed a consistent relationship between retrieved EWT and canopy water content for the different simulated architectural scenarios. It was shown that EWT was negatively affected by leaf dry matter and soil background. Retrievals of EWT from hyperspectral *Advanced Visible Infrared Imaging Spectrometer* (AVIRIS) imagery at three study sites were then used for cross-validation of the *Moderate Resolution Imaging Spectrometer* (MODIS) data, assessing the behavior of NDVI, EVI, NDWI, and SIWSI as potential indicators of vegetation water content. All four MODIS indexes showed consistent agreement with retrievals of EWT from AVIRIS imagery at the agricultural site and the savanna–shrub site, with EVI having the highest correlation. However, at the conifer forest study site the two water indexes, NDWI and SIWSI, yielded better agreement with retrievals of EWT than NDVI and EVI. The performance of NDVI was inconsistent across sites. This manuscript demonstrates the importance of canopy architecture when estimating EWT by showing that large errors are obtained when EWT estimates derived from absorption feature curve-fitting are applied to different canopy types. These errors are propagated in simple indexes that produce inconsistent results when applied to divergent vegetation conditions.

Keywords: Radiative transfer model; Equivalent water thickness; AVIRIS; MODIS

1. Introduction

Accurate quantitative estimates of biochemical properties of vegetation canopies are important applications of remote sensing for terrestrial ecology (Gao & Goetz, 1995). Estimates of vegetation water content are of interest for assessing vegetation water status in agriculture and forestry (Gao, 1996; Gao & Goetz, 1995; Peñuelas et al., 1997; Ustin et al., 2004a,b, 1998; Zarco-Tejada et al., 2003), and have been used for drought assessment (Peñuelas et al., 1993) and prediction of susceptibility to wildfire (Chuvieco et al., 2004; Riaño et al., 2005; Ustin et al., 1998).

Reflectance in the near-infrared (NIR) and shortwave-infrared (SWIR) regions is largely influenced by water and dry matter in the leaves (Gao, 1996; Jacquemoud et al., 1996; Peñuelas et al., 1997; Tucker, 1980), while photosynthetic pigments only absorb in the visible and red-edge spectral region (Carter, 1994; Miller et al., 1990; Ustin et al., 2004a,b; Zarco-Tejada et al., 2004, 2001). Thus, measurements in NIR-SWIR provide a pigment-independent quantitative estimate of vegetation water content, although they are also affected by leaf structure, leaf dry matter, canopy structure, and leaf area index (Gao, 1996; Jacquemoud et al., 1996; Serrano et al., 2000; Zarco-Tejada et al., 2003). Most satellite and airborne estimates

* Corresponding author.
E-mail address: ybcheng@cstars.ucdavis.edu (Y.-B. Cheng).

0034-4257/$ - see front matter
doi:10.1016/j.rse.2006.07.005

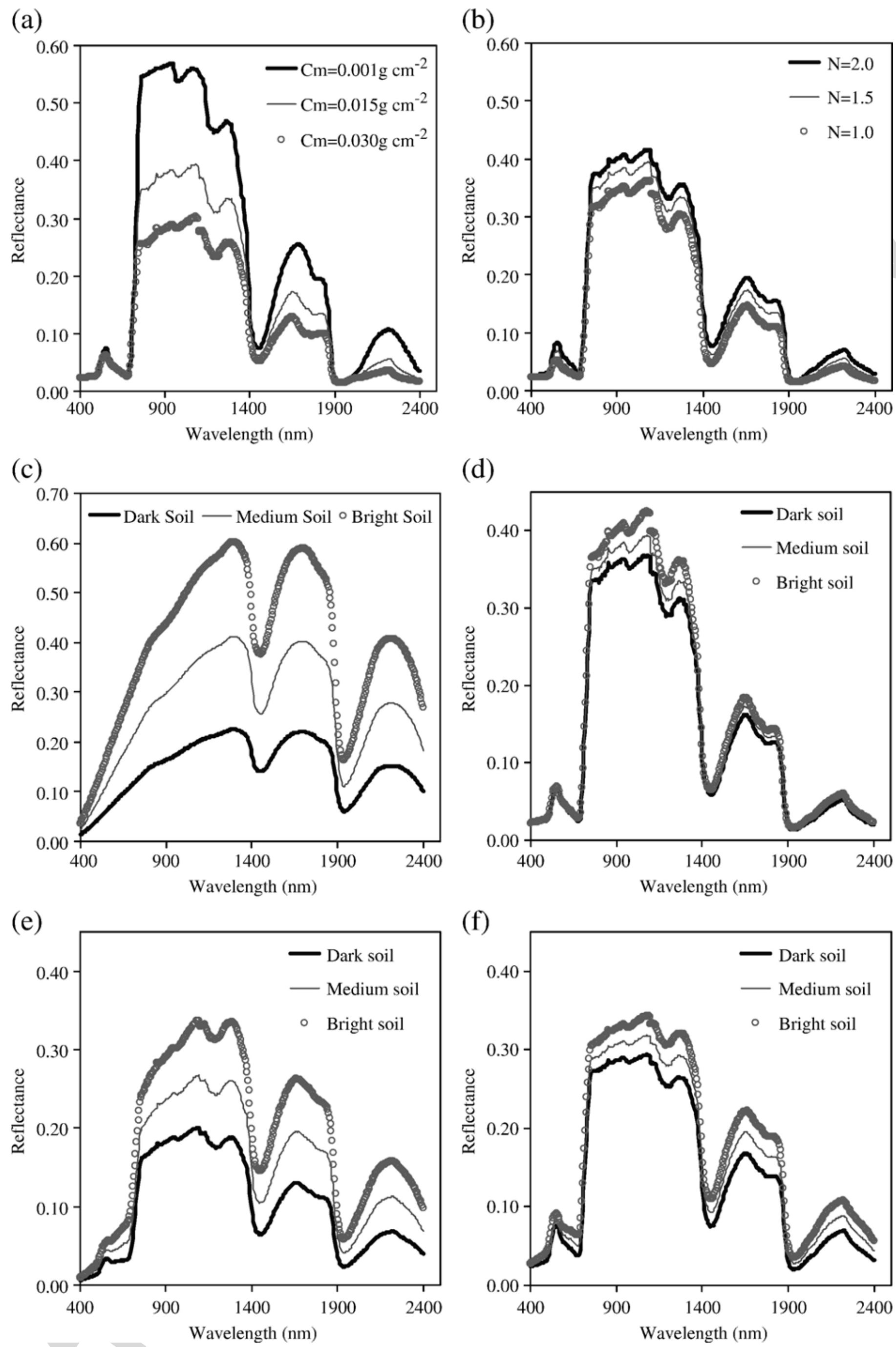

Fig. 1. Effects of (a) dry matter content (C_m) and (b) leaf internal structure parameter (N) on reflectance spectra simulated by PROSPECT-SAILH. (c) Three different soil spectra used in simulation. Effects of different soil background on reflectance spectra simulated by (d) PROSPECT-SAILH, (e) PROSPECT-rowMCRM, (f) PROSPECT-FLIM. (Parameters were set according to Table 1, but leaf equivalent water thickness (C_w) = 0.015 cm, leaf area index (LAI) = 3, sun zenith angle (t_s) = 30°, view zenith angle (t_v) = 0°, and relative azimuth angle (p_s) = 0°).

of vegetation moisture content use empirical band-ratio indexes (Gao, 1996; Huete et al., 1997; Peñuelas et al., 1997; Serrano et al., 2000; Ustin et al., 2004a), but the accuracy of these indexes across a wide range of ecological conditions is uncertain.

Several studies support that accurate estimates of canopy water content can be derived from the *Moderate Resolution Imaging Spectrometer* (MODIS). Zarco-Tejada and Ustin (2001) and Zarco-Tejada et al. (2003) proposed a model inversion method with a linked leaf-canopy radiative transfer simulation which successfully monitored water content in chaparral vegetation by taking into account variations in leaf characteristics and canopy structure (Zarco-Tejada et al., 2003). The MODIS data product MOD09A1 provides calibrated reflectance for the seven spectral bands in the 400–2500 nm spectral region that are measured at 250 m or 500 m pixel resolutions (http://modis.gsfc.nasa.gov). Band 2, centered at 858.5 nm, band 5 at 1240 nm, and band 6 at 1640 nm have been used to retrieve water content (Fensholt & Sandholt, 2003; Gao, 1996; Xiao et al., 2005; Zarco-Tejada et al., 2003; Zarco-Tejada & Ustin, 2001). Gao (1996) first proposed the *Normalized Difference Water Index* (NDWI) using the water absorption features at 860 nm and 1240 nm from MODIS to retrieve vegetation liquid water. The combination of MODIS bands centered at 858.5 nm and 1640 nm was proposed under the name of the *Shortwave Infrared Water Stress Index* (SIWSI, Fensholt & Sandholt, 2003) and *Land Surface Water Index* (LSWI, Xiao et al., 2005) to monitor spatial and temporal changes in vegetation water content in the semiarid Sahelian zone of West Africa and paddy rice fields in China. This combination is essentially the same as the *Normalized Difference Infrared Index* (NDII, Hardisky et al., 1983) applied to the Landsat Thematic Mapper data.

In hyperspectral airborne studies, analytical techniques have been developed to interpret water absorption features for vegetation water content estimates (Gao & Goetz, 1995; Green et al., 1993; Roberts et al., 1997; Serrano et al., 2000; Ustin et al., 1998). Given the contiguous spectral coverage in the 400–2500 nm region, a spectral matching technique was developed to simultaneously estimate water vapor and liquid water in a MODTRAN-based radiative transfer model (ACORN, ImSpec LLC, Analytical Imaging and Geophysics LLC, Boulder, CO) (Green et al., 1991, 1993; Roberts et al., 1997). The MODTRAN-based approach implemented in ACORN provides an output layer in which vegetation liquid water content is expressed as the Equivalent Water Thickness (EWT), or the equivalent depth of water in the pixel that is required to fit the water absorption modeled in the calibration procedure (Green et al., 1991, 1993; Roberts et al., 1997). Roberts et al. (1997) used EWT to monitor temporal and spatial variation in water content in herbaceous, shrub, and conifer vegetation. Ustin et al. (1998) compared different methods for estimating canopy water content and showed that EWT could estimate canopy water content of chaparral shrubs and detect seasonal differences. Serrano et al. (2000) reported that EWT showed significant contrast among plant communities of coastal sage shrub, ceanothus, and chamise chaparral. Later, Champagne et al. (2003) validated EWT against *in situ* plant-derived estimates, and demonstrated EWT to monitor plant water content in crops. Cheng et al. (submitted for publication-a) also showed that retrievals of EWT from Advanced Visible Infrared Imaging Spectrometer (AVIRIS) data had good agreement with *in situ* canopy water content measurement at a semi-arid site, although under-estimated canopy water content at plots which contained significant proportions of soil background. Canopy Relative Water Content (RWC) measured in the field (Serrano et al., 2000) was compared to retrievals of EWT from AVIRIS data, which did not perform as well as simple water indexes. Thus, uncertainties introduced by plant physiological and environmental parameters into EWT retrievals derived from the MODTRAN-based curve-fitting method in ACORN need further study.

This study extends progress in understanding and assessing uncertainties of the algorithm for retrieval of EWT implemented in ACORN using three architecturally extreme vegetation scenarios simulated by three radiative transfer (RT) models. First we applied a leaf radiative transfer model to three canopy reflectance models to simulate three different vegetation cover types: (i) closed canopy crops, (ii) row-structured open canopy crops, and (iii) closed canopy forests. The three linked models were used to generate synthetic AVIRIS-equivalent spectra in order to examine the agreement between theoretical vegetation canopy water content and EWT retrievals obtained from the ACORN-based fitting algorithm that have been widely used and accepted for this purpose (Champagne et al., 2003; Cheng et al., submitted for publication-a; Green et al., 1993; Roberts et al., 1997; Serrano et al., 2000; Ustin et al., 1998).

This investigation studied the potential effects of other leaf biochemical and canopy biophysical variables on EWT retrievals using synthetic AVIRIS-equivalent spectra. Furthermore, three study sites with different vegetation types and cover were chosen for comparison, and EWT at the three sites were retrieved from AVIRIS imagery acquired in years 2002 and 2004 with the same algorithm. The EWT maps were resampled to MODIS pixels and compared to four band-ratio indexes derived from MODIS reflectance products to evaluate the agreement of water retrievals from AVIRIS and MODIS instruments with different resolutions.

2. Study sites

Three study sites with different architectural characteristics were selected for this modeling study: (i) closed and open canopy crops, (ii) semi-arid shrublands, and (iii) boreal conifer forests.

Table 1
Values of parameters when they are fixed and range of variation when parameters are randomly generated

	Range of variation	Fixed value
PROSPECT		
Leaf water content, C_w (cm)	0.001–0.03	
Leaf dry matter content, C_m (g cm^{-2})	0.001–0.03	0.015
Leaf internal structure parameter, N	1–2	1.5
SAILH		
Leaf area index, LAI	1–5	
Leaf angle distribution function, LADF	Planophile, erectophile, plagiophile	Plagiophile
Soil reflectance, ρ_s	Bright, medium, dark	Medium
rowMCRM		
Leaf area index, LAI	1–5	
Leaf angle distributeion function, LADF	Planophile, erectophile, plagiophile	Plagiophile
Soil reflectance, ρ_s	Bright, medium, dark	Medium
Canopy height, h	0.2–2	1.1
Crown width, lp	0.2–1.5	0.85
Soil strip length, ls	0.2–2	1.1
Row direction, alpha row	0–180	90
FLIM		
Leaf area index, LAI	1–5	
Leaf angle distribution function, LADF		
Soil reflectance, ρ_s	Bright, medium, dark	Medium
Crown height (m)	5–20	12.5
Crown diameter (m)	3–8	5.5
Tree density (trees ha^{-1})	200–1000	500
Extinction coefficient of crown, crown alpha	0.3–0.7	0.5

The first site is located at AZCAL Properties in the San Joaquin Valley (36°13′14″N, 119°55′55″W) near Lemoore, California (USA), approximately intermediate between Los Angeles and San Francisco. Seven common agricultural crops (alfalfa, cotton, tomatoes, garlic, wheat, beans, and carrots) are produced on the ranch, and all but the pistachio orchards have crops rotated annually among fields. The crop map for the section of the ranch used in this study was previously described by Ustin et al. (2004a). We selected alcala (*Gossypium hirsutum* L.) and pima (*Gossypium barbadense* L.) cotton fields to analyze, each averaging 67 ha for a total of 871 ha, and the average yield of these fields was 6010 kg/ha in 2002.

The second site, Walnut Gulch Experimental Watershed, is a USDA research station and AmeriFlux site located near Tombstone in southeastern Arizona (USA) (Hymer et al., 2000; Huete et al., 2002). Walnut Gulch (centered at 31°44′12″N and 109°56′31″W) is located within the upper 150 km^2 of the San Pedro River drainage basin. In the past, most of this semi-arid site was covered by grassland, but shrubs now dominate two thirds of the watershed (Abrahams et al., 1995; Hymer et al., 2000; Huete et al., 2002; http://www.tucson.ars.ag.gov). Creosote bush (*Larrea tridentata*), whitethorn (*Acacia constricta*), and banana yucca (*Yucca baccata*) are the most common shrubs in the shrubland region while the grassland located east of the shrubland is dominated by black grama (*Bouteloua eripoda*), curly mesquite grass (*Hilaria belangeri*), and tobosa grass (*Hilaria mutica*) (Abrahams et al., 1995; Hymer et al., 2000).

The third site selected is the Howland Forest, an AmeriFlux research site and EOS land validation core site of 7000 ha centered around 45°12′33″N and 68°44′49″W, located north of Bangor, Maine (USA) (Hollinger et al., 2004, 1999; http://www.geog.umd.edu/cress/s8rep.htm). This boreal transition forest consists of spruce–hemlock–fir, aspen–birch, and hemlock–hardwood mixtures, and is dominated by red spruce (*Picea rubens* Sarg.) and eastern hemlock (*Tsuga canadensis* (L.) Carr.) around the flux measurement tower (Hollinger et al., 2004, 1999).

3. Simulation methods and image data processing

3.1. Models simulation methods

The widely used leaf radiative transfer model, PROSPECT (Jacquemoud, 1993; Jacquemoud & Baret, 1990; Jacquemoud et al., 1995, 1996), was linked with three different canopy reflectance models: (i) SAILH (Kuusk, 1985; Verhoef, 1984) to simulate a closed crop scenario; (ii) rowMCRM, a *Markov-Chain Canopy Reflectance Model* (MCRM) (Kuusk, 1995a,b) with additions to simulate row crop structure; and (iii) FLIM (Rosema et al., 1992) to simulate open-canopy woodlands. For the FLIM model, leaf reflectance (ρ) and transmittance (τ) spectra from PROSPECT were used as inputs since the FLIM model requires an infinite reflectance (ρ_{canopy}) for the simulation of the crown reflectance. The Lillesaeter model (Lillesaeter, 1982) designed for an infinite number of stacked

Table 2
Effects of leaf and canopy parameters on retrieval of EWT from ACORN as shown by the coefficient of determination (r^2)

Randomly generated parameters	*C*w, LAI			*C*w, LAI, C_m			*C*w, LAI, *N*			*C*w, LAI, LADF			*C*w, LAI, ρ_s			*C*w, LAI, *h* (crown_h)			*C*w, LAI, lp (crown_d)			*C*w, LAI, ls (tree_D)		
Sun zenith angle	**15**	**30**	**55**	**15**	**30**	**55**	**15**	**30**	**55**	**15**	**30**	**55**	**15**	**30**	**55**	**15**	**30**	**55**	**15**	**30**	**55**	**15**	**30**	**55**
PROSPECT+ SAILH	*0.96*	*0.97*	*0.96*	*0.89*	*0.91*	*0.89*	*0.94*	*0.94*	*0.94*	*0.94*	*0.94*	*0.95*	*0.95*	*0.95*	*0.95*									
PROSPECT+ rowMCRM	*0.96*	*0.92*	*0.90*	*0.82*	*0.86*	*0.87*	*0.96*	*0.93*	*0.90*	*0.95*	*0.93*	*0.90*	*0.79*	*0.83*	*0.90*	*0.91*	*0.68*	*0.76*	*0.60*	*0.64*	*0.87*	*0.45*	*0.48*	*0.84*
PROSPECT+ FLIM	*0.89*	*0.88*	*0.86*	*0.80*	*0.77*	*0.70*	*0.77*	*0.79*	*0.72*				*0.76*	*0.82*	*0.86*	*0.88*	*0.88*	*0.85*	*0.67*	*0.71*	*0.76*	*0.73*	*0.74*	*0.81*

Randomly generated parameters	*C*w, LAI, alpharow			*C*w, LAI, crown_alpha			*C*w, LAI, *C*m, *N*			*C*w, LAI, LADF, ρ_s			*C*w, LAI, and canopy			*C*w, LAI, leaf and canopy		
Sun zenith angle	**15**	**30**	**55**	**15**	**30**	**55**	**15**	**30**	**55**	**15**	**30**	**55**	**15**	**30**	**55**	**15**	**30**	**55**
PROSPECT+ SAILH							*0.90*	*0.88*	*0.88*	*0.93*	*0.93*	*0.93*				0.86	0.87	0.86
PROSPECT+ rowMCRM	*0.95*	*0.85*	*0.69*				*0.82*	*0.85*	*0.87*	*0.79*	*0.82*	*0.90*	*0.36*	*0.41*	*0.42*	*0.36*	*0.37*	*0.49*
PROSPECT+ FLIM				*0.86*	*0.87*	*0.88*	*0.73*	*0.71*	*0.63*				*0.68*	*0.71*	*0.76*	*0.63*	*0.62*	*0.64*

Bold fonts indicate sun zenith angle. Italic fonts indicated r^2 of *C*w*LAI and EWT.
C_w, LAI, and canopy parameters:
PROSPECT-rowMCRM: *C*w, LAI, LADF, ρ_s, *h*, lp, ls, alpharow.
PROSPECT-FLIM: *C*w, LAI, ρ_s, tree_D, crown_d, crown_h, crown_alpha.
C_w, LAI, leaf and canopy parameters:
PROSPECT-SAILH: C_w, LAI, C_m, *N*, LADF, ρ_s.
PROSPECT-rowMCRM: C_w, LAI, C_m, *N*, LADF, ρ_s, *h*, lp, ls, alpharow.
PROSPECT-FLIM: C_w, LAI, C_m, *N*, ρ_s, tree_D, crown_d, crown_h, crown alpha.

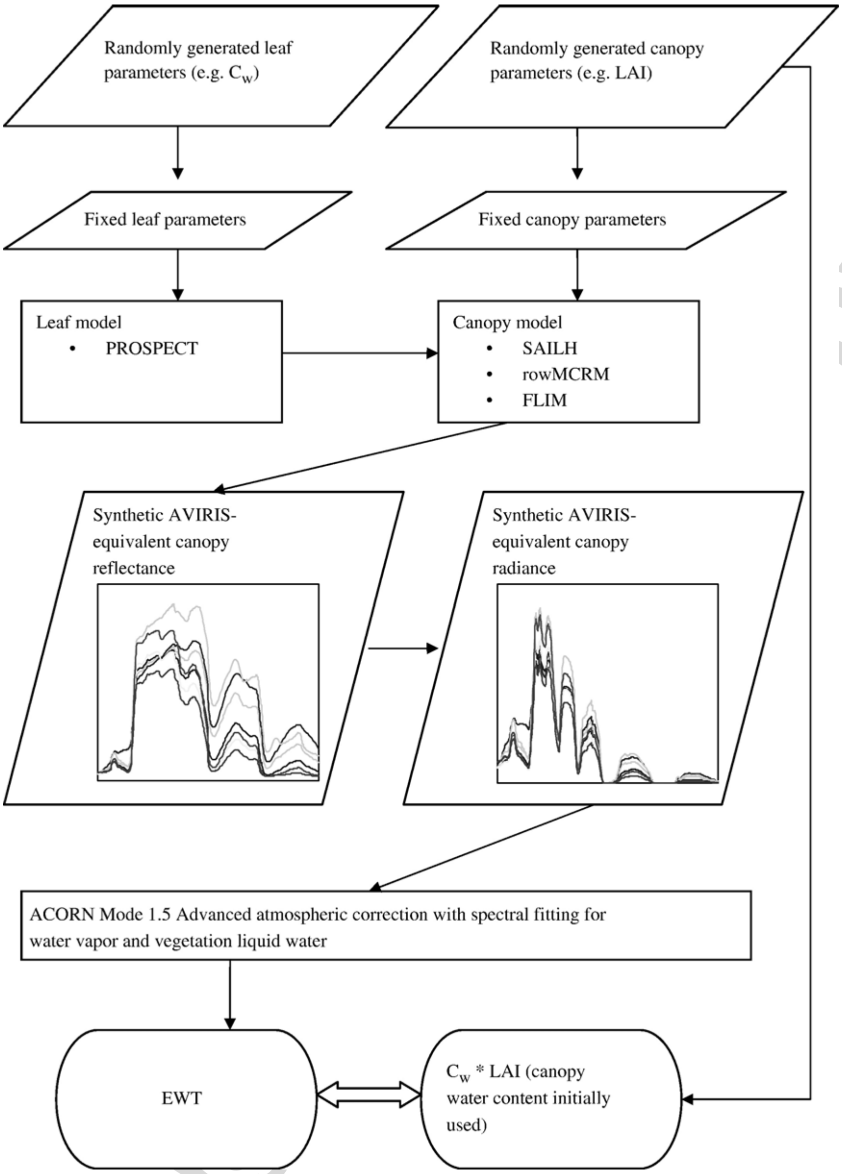

Fig. 2. Schematic view of the simulation study for EWT retrieval.

leaves was linked to FLIM to simulate crown reflectance from PROSPECT leaf optical properties (Eq. (1)).

$$\rho_{\text{canopy}} = \frac{\rho}{1-\tau^2} \quad (1)$$

The simulation of infinite canopy reflectance from leaf reflectance and transmittance has been successfully demonstrated in previously published studies (see Zarco-Tejada et al., 2001). The synthetic spectra generated by the three models (5 nm bandwidth) were later convolved to AVIRIS-equivalent wavelength intervals using band center and Full-Width-Half-Max (FWHM) intervals of the appropriate Gaussian function contained in spectral calibration files of AVIRIS data.

The influences of leaf biochemical and canopy biophysical parameters on the retrievals of EWT by the ACORN fitting method under each canopy scenario were studied using simulations of canopy reflectance by forward modeling. The leaf model, PROSPECT, was randomly varied for inputs such as dry matter content (C_m) and the internal leaf structure parameter (N) since these variations affect water absorption features, which is shown in Fig. 1a and b, respectively. In contrast, variation in chlorophyll content (C_{a+b}) does not affect spectral regions beyond 800 nm and therefore was set to a constant value.

The potential effects of soil background on retrievals of EWT were investigated for each model simulation using three soil reflectance spectra. The three soil spectra (Kuusk, 2001) used as input are shown in Fig. 1c and the synthetic canopy spectra generated by the three linked leaf-canopy models are shown in Fig. 1d–f. For the FLIM model, the three soils were considered as ground reflectance to emphasize the soil background effects. Clearly, these model results demonstrate the contribution of background conditions on water content retrieval as a function of the canopy closure. All simulation

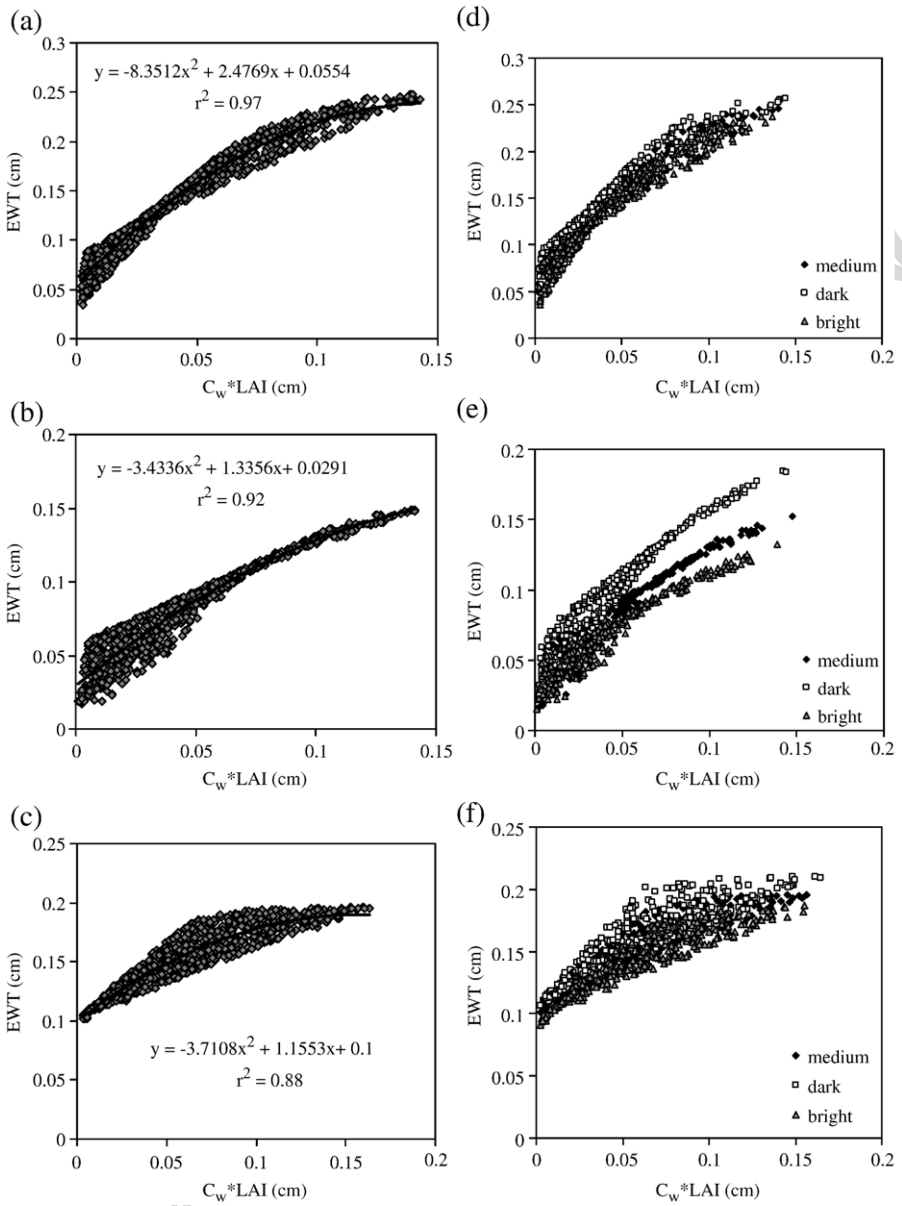

Fig. 3. Correlation between EWT retrieval by ACORN and canopy water content used to simulate spectra with (a) PROSPECT-SAILH, (b) PROSPECT-rowMCRM, (c) PROSPECT-FLIM when C_w and LAI were randomly chosen. Effects of soil background reflectance on regression between EWT retrieval from ACORN and canopy water content used to simulate spectra with (d) PROSPECT-SAILH, (e) PROSPECT-rowMCRM, (f) PROSPECT-FLIM when C_w, LAI, and soil background reflectance were randomly chosen. Other parameters were set at fixed values listed in Table 1. Viewing geometry parameters were set at $t_s=30°$, $t_v=0°$, and $p_s=0°$.

parameters are listed in Table 1 and viewing geometry parameters were set at: sun zenith angles (t_s)=30°, view zenith angle (t_v)=0°, and relative azimuth angle (p_s)=0°.

Each variable that might affect retrievals of EWT was systematically studied. In each case, parameters were generated using a uniform distribution and a subset was chosen randomly within a given range, while others were set to a fixed value. Several previous radiative transfer modeling studies were used to define the ranges (Bacour et al., 2002; Ceccato et al., 2001; Jacquemoud et al., 1996; Zarco-Tejada et al., 2003). The ranges and fixed values are listed in Table 1 and the different cases are listed in Table 2. Eight cases were simulated with PROSPECT-SAILH, 13 cases with PROSPECT-rowMCRM, and 11 cases with PROSPECT-FLIM. Each case consisted of a total of 1000 synthetic AVIRIS-equivalent canopy reflectance spectra, and each case was simulated three times for three different sun zenith angles (t_s) (15°, 30° and 55°). View zenith angle (t_v) and relative azimuth angle (p_s) were both set to 0°. The leaf angle distribution function (LADF) was randomly chosen among planophile, erectophile, and plagiophile distributions (Lemeur, 1970) while soil reflectance was randomly chosen from the three spectra of differing brightness (shown in Fig. 1c). Leaf water content (C_w) and leaf area index (LAI) were the two parameters that were randomly generated in each case since EWT is sensitive to changes in both. The input value of C_w* LAI used for the simulations in the forward modeling scheme was considered the

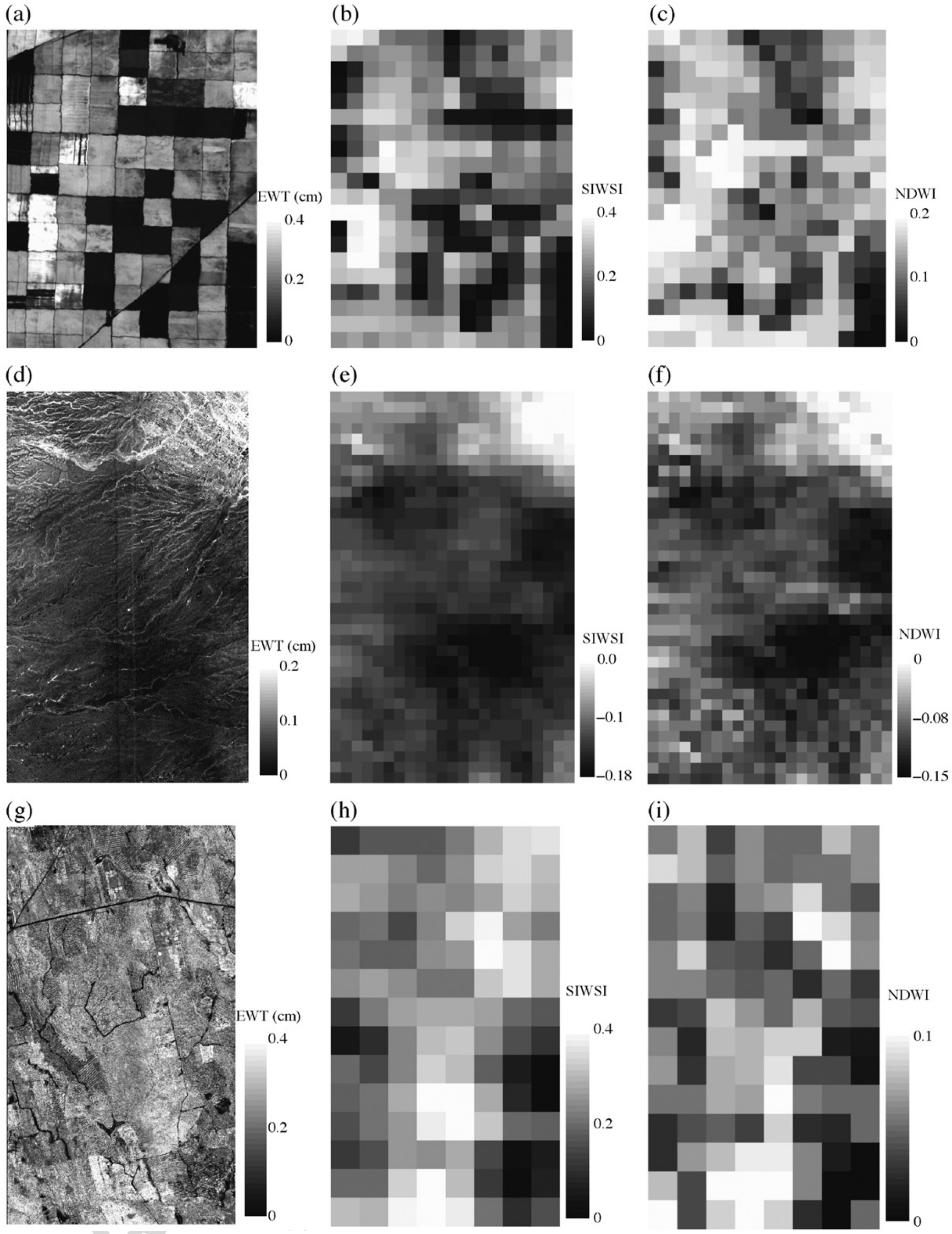

Fig. 4. EWT maps developed from AVIRIS imagery at (a) AZCAL Properties, CA on 16 July 2002, (d) Walnut Gulch, AZ on 25 August 2004, (g) Howland forest, ME on 23 August 2002. SIWSI map developed from MODIS imagery at (b) AZCAL Properties, CA, (e) Walnut Gulch, AZ, (h) Howland forest, ME. NDWI map developed from MODIS imagery at (c) AZCAL Properties, CA, (f) Walnut Gulch, AZ, (i) Howland forest, ME.

"true" canopy water content and used to validate retrievals of EWT using the AVIRIS-equivalent spectra. All random AVIRIS-equivalent synthetic canopy reflectance spectra were inverted and transformed into radiance using irradiance files generated from ACORN at the three sun zenith angles and a visibility of 23 km.

3.2. Equivalent water thickness retrieval with ACORN

Retrievals of EWT used the ACORN fitting algorithm which integrates techniques developed by Green et al. (1991, 1993) and Roberts et al. (1997). The technique was originally developed to improve water vapor retrieval from AVIRIS data by fitting AVIRIS measured radiance centered at 940 nm to a radiance spectrum of water vapor absorption generated by ACORN. Because of a 40 nm spectral difference between the center wavelength of liquid water absorption and water vapor absorption, liquid water can be simultaneously retrieved with water vapor by fitting the measured pixel reflectance to the equivalent transmittance spectrum for a slab of water based on the Beer-Lambert Law (Green et al., 1993; Roberts et al., 1998, 1997). Although this technique was originally designed to improve water vapor compensation for calibrating AVIRIS data to apparent surface reflectance, studies have shown the potential to retrieve this physically based liquid water feature and use it to monitor vegetation water content (Champagne et al., 2003; Cheng et al., submitted for publication-a; Roberts et al., 1997; Serrano et al., 2000; Ustin et al., 1998). Cheng et al. (submitted for publication-b) showed that EWT from AVIRIS was linearly related to spectral water indexes. Retrievals of EWT were made from all synthetic AVIRIS-equivalent radiances using ACORN and the retrieved EWT was later compared with canopy water content used as input for the simulations under the different canopy scene assumptions and variation of leaf and canopy parameters. The schematic view of the simulation study to retrieve EWT from simulated spectra is shown in Fig. 2.

3.3. Validation of retrievals from AVIRIS and MODIS imagery

The AVIRIS instrument is an airborne high-spatial resolution hyperspectral scanner, having 224 contiguous bands in 400–2500 nm with approximately 10 nm bandwidth. AVIRIS spatial resolution varies from 4 m to 20 m depending on flight altitude. An atmospheric correction to convert the data from radiance to apparent surface reflectance was performed using ACORN. EWT was retrieved from AVIRIS data using ACORN Mode 1.5: Advanced atmospheric correction of hyperspectral data with spectral fitting for water vapor and vegetation liquid water. AVIRIS overflights at AZCAL Properties (16 July 2002), Walnut Gulch Experimental Watershed (25 August 2004), and the Howland Forest (23 August 2002) were used to retrieve EWT, which was subsequently used as a reference for canopy water content. After comparison to the simulation study, AVIRIS EWT was used to examine canopy water content retrievals from MODIS products by calculating the mean EWT from AVIRIS data for the area of each MODIS pixel.

The MODIS reflectance product (MOD09A1) is an 8-day composite dataset consisting of seven bands between 400 nm and 2500 nm and six additional bands indicating viewing geometry, state information, and atmospheric conditions. Band 1 (645 nm), Band 2 (858.8 nm), and Band 3 (469 nm) were used to derive the greenness indexes NDVI following Eq. (2) (Rouse et al., 1974) and EVI with Eq. (3) (Huete et al., 2002), respectively. Band 2 (858.5 nm), Band 5 (1240 nm), and Band 6 (1640 nm) were used to calculate the water indexes NDWI and SIWSI following Eq. (4) (Gao, 1996; Zarco-Tejada et al., 2003) and Eq. (5) (Fensholt and Sandholt, 2003), respectively.

$$\mathrm{NDVI} = \frac{\mathrm{Band2}-\mathrm{Band1}}{\mathrm{Band2}+\mathrm{Band1}} = \frac{R_{858.5}-R_{645}}{R_{858.5}+R_{645}} \tag{2}$$

$$\begin{aligned}\mathrm{EVI} &= 2.5 \times \frac{\mathrm{Band2}-\mathrm{Band1}}{\mathrm{Band2}+6\times\mathrm{Band1}-7.5\times\mathrm{Band3}+1} \\ &= 2.5 \times \frac{R_{858.5}-R_{645}}{R_{858.5}+6\times R_{645}-7.5\times R_{469}+1}\end{aligned} \tag{3}$$

$$\mathrm{NDWI} = \frac{\mathrm{Band2}-\mathrm{Band5}}{\mathrm{Band2}+\mathrm{Band5}} = \frac{R_{858.5}-R_{1240}}{R_{858.5}+R_{1240}} \tag{4}$$

$$\mathrm{SIWSI} = \frac{\mathrm{Band2}-\mathrm{Band6}}{\mathrm{Band2}+\mathrm{Band6}} = \frac{R_{858.5}-R_{1640}}{R_{858.5}+R_{1640}} \tag{5}$$

MODIS data were cross-calibrated to AVIRIS data to align the radiometric measurements (accounting for view geometry differences due to swath position and the 8-day compositing). AVIRIS was spatially and spectrally degraded to match MODIS resolutions and bright pixels (e.g. vegetation, like cotton fields in the near-infrared region) and dark pixels (e.g. harvested areas and bare soil) were chosen from each image to develop an empirical cross-calibration regression for each spectral band. AVIRIS pixels within the corresponding MODIS pixel were extracted as mean reflectance for MODIS Band 1, Band 2, Band 3, Band 5 and Band 6 over the full extent of the AVIRIS overflights.

3.4. Statistical analysis

For each of the four MODIS indexes, consistency of regressions with AVIRIS EWT at different sites was examined by testing parallelism between two straight regression lines. The test for parallelism (Kleinbaum et al., 1988) was performed on two regression lines of AVIRIS and one MODIS index at different study sites. This involved a null hypothesis of no difference between the two slopes from two regression lines of AVIRIS EWT and one MODIS index at two different sites, and α value was set as 0.05 in this study. The test statistic was computed as the difference between the two slopes divided by the standard error of the difference between the slopes.

4. Results

4.1. Retrieval of EWT from synthetic spectra

Retrievals of EWT from ACORN were conducted using randomly chosen synthetic canopy reflectance spectra from each of the three models. These EWT retrievals were compared to the product of C_w and LAI used as inputs and the resulting determination coefficients are provided in Table 2. Results show that retrievals of EWT from ACORN-simulated spectra produced good relationships to actual canopy water content derived from input data used to generate the synthetic canopy reflectance spectra for the linked leaf-canopy models (r^2=0.86–0.97). Modeled EWT, with the exception of the canopy properties for rowMCRM, have r^2=0.60 or better.

The regression results when C_w and LAI only were randomly generated are shown in Fig. 3a,b,c. The determination coefficient between retrieved EWT and canopy water decreases as more parameters are included in the model (Table 2). At the

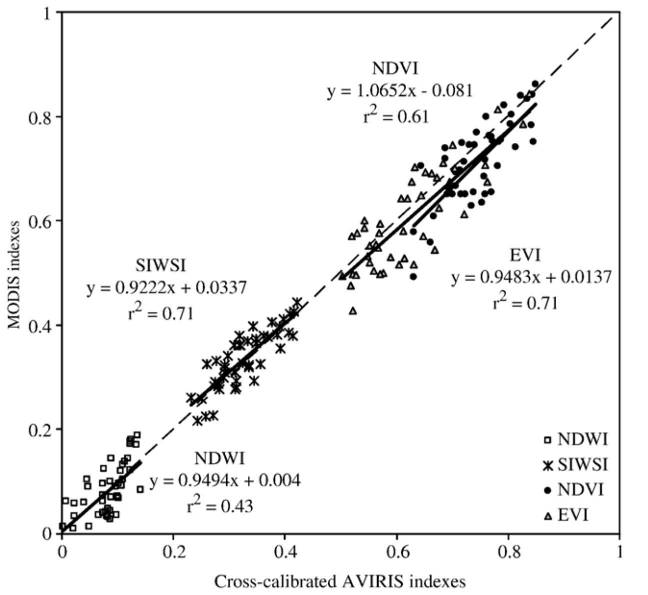

Fig. 5. Comparison of four indexes derived from MODIS reflectance product and cross-calibrated AVIRIS data at AZCAL Properties, CA on 16 July 2002.

leaf level, all three linked leaf-canopy models show that changes in dry matter content (C_m) decreased values of r^2 more than the internal structure parameter (N). This result indicates that changes in dry matter should produce more errors in retrievals of EWT than the number of layers a leaf is composed of. At the canopy level, the contribution of background soil reflectance was observed in all three models. However, it was more significant in open canopies with direct background contributions than in closed-canopy uniform vegetation, as expected. The three different soil backgrounds used in the synthetic canopy reflectance spectra are distinguishable in regressions between retrieved EWT and input canopy water content (Fig. 3d–f). With the same input canopy water content, the synthetic canopy reflectances simulated with dark soils retrieved highest EWT, which is lower in medium and bright soils (Fig. 3d–f). This discrimination is most apparent in cases simulated from the PROSPECT-rowMCRM model (Fig. 3e) than from the other two models. The three sun zenith angles (15°, 30°, and 55°) used in this study show that in most cases there was little influence on the correlation coefficients for EWT (Table 2). Overall, these results indicate the importance of the canopy structure and background component influences on estimates of EWT from the widely accepted MODTRAN-based curve-fitting method in ACORN.

4.2. Comparison of AVIRIS and MODIS data for water content estimation

Given the acceptably high r^2 (mean = 0.79; n = 96) considering all simulations between modeled water content and retrievals of EWT using ACORN, we investigated the retrieval of canopy water content from MODIS by comparing EWT retrieved from AVIRIS to four vegetation/water indexes derived from MODIS reflectance data at the three study sites. The ACORN-derived EWT developed from AVIRIS imagery at the three study sites at the original AVIRIS spatial scale are shown in Fig. 4a (AZCAL Properties), d (Walnut Gulch), and g (Howland Forest). One MODIS image was coincident with each AVIRIS overflight. The corresponding SIWSI and NDWI were derived from MODIS MOD09A1 reflectance, shown in Fig. 4b,e,h and c,f,i, respectively.

Before comparing the AVIRIS EWT to the MODIS indexes, the AVIRIS and MODIS indexes were cross-calibrated. The four indexes (NDVI, EVI, NDWI, and SIWSI) were calculated to assess data agreement. MODIS band-passes and spatial resolutions were computed in AVIRIS data. Fig. 5 shows the four indexes derived from AVIRIS and MODIS data at AZCAL Properties on 16 July 2002. The regression between AVIRIS NDWI and MODIS NDWI was close to the one-to-one relationship. This agreement between AVIRIS and MODIS indexes was previously shown at an old-growth conifer forest in southwestern Washington (Cheng et al., submitted for publication-b). Based on this agreement, comparisons between ACORN-derived EWT from AVIRIS data and indexes derived from MODIS MOD09A1 reflectance bands were then conducted.

4.3. Comparisons between AVIRIS EWT and MODIS indexes

The four NDVI, EVI, NDWI, and SIWSI indexes calculated from MODIS MOD09A1 reflectance consistently had linear relationships to ACORN-derived EWT from AVIRIS at all three study sites. The sites varied about one order of magnitude in EWT although the mean EWT was markedly different, with Walnut Gulch having an order of magnitude lower EWT than AZCAL or Howland. Likewise the magnitude and ranges of the four indexes varied widely between the three sites. In general, the range of values for a particular index within each site was not large. The regressions between AVIRIS EWT and the MODIS indexes are shown in Fig. 6 and Table 3.

At AZCAL Properties, all four indexes showed similar correlations to retrievals of EWT. MODIS EVI had the best r^2 at 0.64 while MODIS NDVI was slightly lower at r^2 = 0.50 (Fig. 6, Table 3), as expected. The water indexes were intermediate between the chlorophyll indexes, with NDWI r^2 = 0.54 and

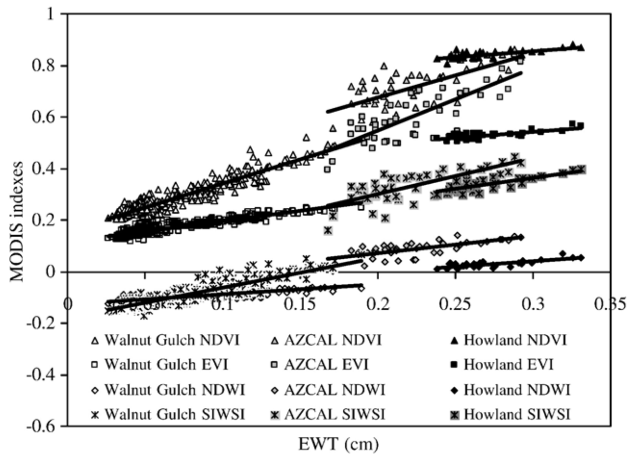

Fig. 6. Regression between four indexes derived from MODIS data and EWT retrieved from AVIRIS imagery at AZCAL Properties, CA on 16 July 2002, Walnut Gulch, AZ on 25 August 2004, Howland forest, ME on 23 August 2002.

Table 3
Statistics of regressions between AVIRIS EWT and MODIS indexes presented in Fig. 6

MODIS indexes (y)	AVIRIS EWT (cm) (x)								
	Walnut Gulch			AZCAL Properties			Howland Forest		
	a	b	r^2	a	b	r^2	a	b	r^2
NDVI	1.887	0.1528	0.89	1.7065	0.3348	0.50	0.4569	0.7182	0.49
EVI	0.8126	0.1146	0.82	2.4188	0.0624	0.64	0.4576	0.405	0.55
NDWI	0.3903	0.129	0.62	0.7014	0.0701	0.54	0.4067	0.0821	0.59
SIWSI	1.1655	0.1807	0.81	1.415	0.0173	0.57	0.8491	0.11	0.66

Regression line: $y=ax+b$

SIWSI $r^2=0.57$. These data (day 197) were acquired 2–3 weeks after canopy closure (LAI ~ 2–2.5) at a time when the canopy is fully green and growing exponentially.

In the Walnut Gulch region, all four MODIS indexes yielded good correlations (the highest correlations among the three sites) with ACORN-derived EWT from AVIRIS imagery. MODIS NDVI obtained the best r^2 at 0.89 to retrievals of EWT followed by EVI with $r^2=0.82$ and SIWSI at $r^2=0.81$, while NDWI had the lowest correlation with $r^2=0.62$ (Fig. 6b; Table 3). The data from this site was acquired about 2 weeks after the start of the summer monsoon in 2004. One explanation for the larger range in NDVI at this site and the higher correlations to all indexes despite the low EWT is due to the rapid response of the grasslands to the summer precipitation while the creosote bush community was mostly dormant and showed little response to summer rain. LAIs for these discontinuous canopy vegetation types range from 0.16 to 0.3 (Cheng et al., submitted for publication-a).

At Howland forest, the two water indexes derived from MODIS data had better correlations to EWT ($r^2=0.66$ for SIWSI and 0.59 for NDWI). Here, the two MODIS vegetation indexes performed less well, NDVI had the lowest correlation to EWT with r^2 of 0.49, and EVI having a slightly better correlation ($r^2=0.55$) than NDVI. LAI at this Ameriflux site is reported an average of 5.5 (Hollinger et al., 1999), putting it in the range where NDVI is typically saturated (Holben et al., 1980; Sellers, 1985), possibly explaining the lower correlation for the vegetation indexes. Other dense conifer forests have also shown that water indexes provide better estimates of LAI than NDVI (Roberts et al., 2004).

Statistical analysis showed that for each MODIS index, its regression lines with ACORN-derived EWT from AVIRIS were not consistently parallel among the sites. For NDVI and SIWSI, slopes of regression lines with EWT were significantly different at the forest site, Howland. For EVI and NDWI, slopes of regression lines were significant at the agricultural site, AZCAL Properties.

5. Discussion

Three linked leaf-canopy radiative transfer models having different vegetation canopy closure scenarios were used to generate AVIRIS-equivalent spectra. Possible model errors and uncertainties in estimates of water content due to covarying leaf biochemical and canopy biophysical properties were tested as shown in Table 2. At the leaf level, variation in dry matter produces the largest error in water content. At the canopy level varying soil brightness had a large effect on the PROSPECT-rowMCRM model. All models show decreasing accuracy as the number of independent parameters that are allowed to vary increases. The variation in retrieval accuracy of ACORN-derived EWT is shown by the coefficients of determination in Table 2, which varied from 0.36 to 0.97. When only leaf water content (C_w) and LAI were allowed to vary, good correlation ($r^2=0.86$–0.97) was achieved between simulated EWT from ACORN and input canopy water content. This demonstrates that ACORN-derived EWT is sensitive to changes in canopy water content and can be used to estimate canopy water content in the three simulated vegetation scenarios when each canopy type is analyzed separately. This is illustrated in Fig. 3 which shows that retrievals of EWT are significantly influenced by vegetation canopy architecture causing an over or under estimation of canopy water content.

Nevertheless, different assumptions and algorithms used in these three canopy reflectance models could contribute to the offset and different scattering seen in Fig. 3. For example, dissimilarities in the near-infrared region of spectra generated from SAIL and MCRM were addressed by Bacour et al. (2002) who attributed model differences to how multiple scattering is accounted for. Furthermore, since leaf water content (C_w) and LAI were set to vary independently, low canopy water content could have resulted from either low C_w or low LAI. Thus, the offset seen in Fig. 3 could also have resulted from this and other fixed parameters like dry matter content and soil background reflectance when canopy water content was low.

Our objectives were to investigate the uncertainties in retrievals of EWT, and therefore, changes in correlation with water content used for the simulations due to other variables are emphasized. At the leaf level, as described in the previous section, changes in dry matter content produce more errors in EWT than other leaf biochemical properties. Studies have reported extensive influences caused by both dry matter content (C_m) and leaf internal structure parameter (N) on reflectance in the near- and mid-infrared region simulated by PROSPECT (Bacour et al., 2002; Ceccato et al., 2001). In this study, Fig. 1a,b demonstrate more significant changes in leaf reflectance are introduced by changes of C_m than by N. Nonetheless, dry matter content is usually species-dependent (Riaño et al., 2005; Shipley & Vu, 2001) and might not change as much as in the simulation if only one species type was involved. Therefore, errors contributed by dry matter to EWT could be reduced. At the canopy level, large effects contributed by the soil background were significant although their influence could be determined by estimating the proportions of bare soil and soil background reflectance.

Parameters driving the background proportions of bare soil (e.g. soil strip length in rowMCRM and tree crown diameter in FLIM) affected the retrieval of EWT from ACORN (Table 2). SAILH assumed an idealized canopy layer morphology with a homogenous distribution of horizontal leaves. Therefore, SAILH is more suitable to simulate closed canopy vegetation (e.g. the cotton canopy). Furthermore, because it does not have an explicit parameter for variable soil background, it is less suited for discontinuous canopy conditions such as at the Walnut Gulch site. The proportion of soil background is implicitly accounted for in

SAILH with LAI and LADF parameters, unlike rowMCRM and FLIM. The effect of soil background reflectance for this model is observed in the case where soil background reflectance was randomly chosen and vegetation had low LAI (Fig. 3d).

As we mentioned in the previous section, effects contributed by the soil background reflectance were model-dependent (Fig. 3d–f) and as a function of the amount of each scene component, shadow, background, and pure vegetation, on the simulated architecture reflectance. These differences resulted from differences in the algorithms and assumptions of the three canopy reflectance models. The rowMCRM canopy reflectance model was designed to simulate row-structured canopies (homogenous discontinuously covered canopy). Additionally, based on the random input parameters (crown width and soil strip length), the Fractional Vegetation Cover (FVC) of our PROSPECT-rowMCRM simulation averaged 0.48. Therefore, soil background effects on canopy reflectance are more significant than in the SAILH and FLIM canopy models. As a result, the regression between EWT from ACORN and canopy water content used as input for simulations was largely dependent on soil reflectance (Fig. 3e). In contrast, SAILH and FLIM were designed to simulate vegetation cover scenarios with smaller proportions of bare soil (closed canopy crops and forest), and therefore, soil background reflectance had less effect on these simulations (Fig. 3d,f). Besides, average FVC for PROSEPCT-FLIM simulation was 0.70 based on input parameters (crown width and tree density). Results are therefore consistent, showing larger background effects on the row-structured simulated architecture than in the closed canopies, where soil reflectance plays a minor role.

In the case studies, we extend this understanding of the factors introducing errors into estimates of EWT to evaluate the accuracy of retrievals of canopy water content from MODIS reflectance products using ACORN-derived EWT from AVIRIS imagery. At the AZCAL Properties site, the cotton fields were uniformly closed canopy, mostly green, and with little bare soil and dry plant litter at the growth stage when the AVIRIS image was acquired (16 July 2002). The cotton canopy structure was very similar to the scenario (Table 2) using PROSPECT-SAILH, in which ACORN-derived EWT had the best agreement with actual canopy water content compared to the other two scenarios (Table 2). Therefore, ACORN-derived EWT from AVIRIS imagery should provide the most accurate estimates of canopy water content at the AZCAL site. The two MODIS moisture indexes (NDWI and SIWSI) had similar correlations ($r^2=0.54$ and 0.57) with canopy EWT from AVIRIS imagery. Moreover, the slope of the regression line between EWT and NDWI at the AZCAL site was significantly different from the other two sites. This might suggest a potential usage of NDWI to differentiate agricultural sites. Chlorophyll-based MODIS indexes, NDVI and EVI, also showed similarly good correlations with EWT ($r^2=0.64$ and 0.50). Ustin et al. (2004a) also found NDVI and NDWI had high correlation to measured water content at this site in July 2002, where they estimated water content from AVIRIS by continuum removal at 980 nm (980 CR). While the spectral absorptance of chlorophyll is insensitive to variation in water content, in cotton canopies both water and chlorophyll are co-located in leaves and there is little non-green canopy at this stage in the growing season. Thus LAI is highly correlated with these indexes. The two water measurement indexes, 980 CR and NDWI, are also highly correlated, as expected. Our results are comparable and suggest that retrievals from MODIS products can be used to estimate canopy water content under different canopy types.

In the semi-arid savanna-shrubland at the Walnut Gulch site, MODIS indexes had the best correlation with retrievals of EWT from AVIRIS imagery at the three sites. In contrast to the other sites, vegetation cover is sparse with variable and significant bare soil background and abundant dead plant material. Therefore, within one MODIS pixel (500 m by 500 m), the reflectance is a mixture of green, senescent and dead vegetation, and bare soil. The growth form (grass, shrub) is also expected to vary within MODIS pixels. However, retrievals from MODIS provided good agreement with retrievals from fine spatial resolution AVIRIS data (20 m by 20 m). Because of this mixing, one should assume that EWT from AVIRIS at this site are adversely affected by the variable and abundant soil background reflectance and the varying dry plant matter in the data.

At Howland forest, a conifer and mixed forest, the two MODIS water indexes (NDWI and SIWSI) produced the best correlations with EWT from AVIRIS compared to the two vegetation indexes (NDVI and EVI). Cheng et al. (submitted for publication-b) showed similar results for a Douglas fir/western hemlock-dominated conifer forest in southwestern Washington, where MODIS water indexes (NDWI and SIWSI) had better correlations to EWT than MODIS NDVI. NDVI and EVI do not directly measure water absorptance and become saturated at high leaf biomass typical of dense conifer forests. Roberts et al. (2004) found that NDVI in the Wind River forest in southwestern Washington became insensitive to spatial variation of Leaf Area Index and EWT was better correlated with LAI. Moreover, this might also explain the significantly different slope of the regression line (relatively shallow) between EWT and NDVI at the Howland site. EVI showed higher correlation ($r^2=0.55$) with EWT than NDVI, which might have resulted from its continuing sensitivity to canopy structure at higher LAI (Huete et al., 2002) rather than pigment content.

6. Conclusions

In this study, we investigated a physically-based water index retrieved from hyperspectral AVIRIS images using synthetic spectra from three canopy reflectance models coupled to the PROSPECT leaf radiative transfer model. EWT from simulated AVIRIS data showed good agreement to the input canopy water content from the models. The modeling component of this study showed that while EWT can be used to estimate canopy water content, the presence of leaf dry matter, variation in soil background reflectance, and canopy architecture will contribute errors in EWT retrieval. Four different vegetation/water indexes were derived from MODIS reflectance data and were compared to ACORN-derived EWT from AVIRIS overflights as references at three sites with different vegetation cover. The linear relationship between AVIRIS indexes and MODIS indexes illustrates the general agreement between MODIS and hyperspectral canopy water content retrievals. Indexes derived from MODIS data produced linear correlations with EWT at all three sites (r^2 from 0.49 to 0.89).

At the agricultural site the coefficient of determination for water indexes were in between the correlation to pigment indexes, while at the semi-arid shrub–grassland, the two pigment indexes were highest and the water indexes were lowest, although there was no significant difference between EVI and SIWSI. NDWI had the poorest regression coefficient at this semi-arid site with EWT. At the forested site, the two water indexes had higher r^2 than the two pigment indexes, with NDVI having the lowest correlation compared to the other three indexes. The two MODIS water indexes, NDWI and SIWSI, maintained good correlations with EWT from AVIRIS, and appear to provide better estimates of canopy water content in dense forests.

Differences in ranges, slopes, and r^2 among regressions of the four MODIS indexes at the three sites show that they each measure some independent information about the canopy. Results from the hyperspectral AVIRIS and multispectral MODIS imagery, which are consistent with the simulation study, demonstrate the importance of canopy architecture in quantitative estimates of vegetation EWT. All methods show large errors when EWT estimates are made across vegetation types with markedly different canopy characteristics. We conclude that quantitative estimates of EWT must be modeled separately with appropriate canopy structures to account for different canopy architectures.

Acknowledgements

Portions of this study were supported by National Aeronautics and Space Administration (NASA) under Grant No. NNG0 4GQ42G “Global Estimation of Canopy Water Content” and Contract No. NAG5-9360 “New EOS Data Products to Improve Biogeochemical Estimates” and support from the Cotton Foundation, #5002-008-00, “Evaluation of Advanced Hyperspectral Remote Sensing for Detection of Cotton Water Stress and Irrigation Refinement”. Financial support was provided to P.J Zarco-Tejada under the “Ramón y Cajal” and “Averroes” Programs from Spain are acknowledged. Financial support to D. Riaño under the “Ramón y Cajal” Program of Ministry of Science and Technology from Spain is acknowledged. The authors gratefully acknowledge S. Jacquemond, W. Verhoef, A. Kuusk, and J. Praks for sharing computer code for leaf and canopy reflectance models. George Scheer (University of California, Davis) and Lawrence Ross (University of California, Davis) are gratefully acknowledged for IT support in this study.

References

Abrahams, A. D., Parsons, A. J., & Wainwright, J. (1995). Effects of vegetation change on interrill runoff and erosion, Walnut Gulch, southern Arizona. *Geomorphology*, *13*, 37−48.

Bacour, C., Jacquemoud, S., Tourbier, Y., Dechmbre, M., & Frangi, J. -P. (2002). Design and analysis of numerical experiments to compare four canopy reflectance models. *Remote Sensing of Environment*, *79*(1), 72−83.

Carter, G. A. (1994). Ratios of leaf reflectances in narrow wavebands as indicators of plant stress. *International Journal of Remote Sensing*, *15*, 697−704.

Ceccato, P., Flasse, S., Tarantola, S., Jacquemond, S., & Grégoire, J. -M. (2001). Detecting vegetation leaf water content using reflectance in the optical domain. *Remote Sensing of Environment*, *77*, 22−33.

Champagne, C. M., Staenz, K., Bannari, A., McNairn, H., & Deguise, J-C. (2003). Validation of a hyperspectral curve-fitting model for the estimation of plant water content of agricultural canopies. *Remote Sensing of Environment*, *87*, 148−160.

Cheng, Y.-B., Ustin, S. L., Riaño, D., & Vanderbilt, V. C. (submitted for publication-a). Water content estimation from hyperspectral images and MODIS indexes in southeastern Arizona. *Submitted to Remote Sensing of Environment*.

Cheng, Y.-B., Zarco-Tejada, P. J., Ustin, S. L., Wharton, S., & Paw U, K. T. (submitted for publication-b). Relationships between MODIS water indexes and tower flux data in an old-growth conifer forest. *Manuscript submitted to Journal of Geophysical Research-Atmospheres*.

Chuvieco, E., Cocero, D., Riaño, D., Martin, P., Martínez-Vega, J., de la Riva, J., et al. (2004). Combining NDVI and Surface Temperature for the estimation of live fuels moisture content in forest fire danger rating. *Remote Sensing of Environment*, *92*(3), 322−331.

Gao, B. -C. (1996). NDWI-A normalized difference water index for remote sensing of vegetation liquid water from space. *Remote Sensing of Environment*, *58*(3), 257−266.

Gao, B. -C., & Goetz, A. F. H. (1995). Retrieval of equivalent water thickness and information related to biochemical components of vegetation canopies from AVIRIS data. *Remote Sensing of Environment*, *52*(3), 155−162.

Green, R. O., Conel, J. E., Margolis, J. S., Bruegge, C. J., & Hoover, G. L. (1991). An inversion algorithm for retrieval of atmospheric and leaf water absorption from AVIRIS radiance with compensation for atmospheric scatting. *Proc. third AVIRIS workshop. JPL Publication*, *Vol. 91-28.* Pasadena, CA: Jet Propulsion Laboratory.

Green, R. O., Conel, J. E., & Roberts, D. A. (1993). Estimation of aerosol optical depth and calculation of apparent surface reflectance from radiance measured by the airborne visible-infrared imaging spectrometer (AVIRIS) using MODTRAN2. *SPIE Conference 1937: Imaging Spectrometry of the Terrestrial Environment, the International Society for Optical Engineering (SPIE), Orlando, FL., 14-15 April*.

Fensholt, R., & Sandholt, I. (2003). Derivation of a shortwave infrared water stress index from MODIS near-and shortwave infrared data in a semiarid environment. *Remote Sensing of Environment*, *87*(1), 111−121.

Hardisky, M. A., Lemas, V., & Smart, R. M. (1983). The influence of soil salinity, growth form, and leaf moisture on the specral reflectance of *Spartina alternifolia* canopies. *Photogrammetric Engineering and Remote Sensing*, *49*, 77−83.

Holben, B. N., Tucker, C. J., & Fan, C. -J. (1980). Spectral assessment of soybean leaf area and leaf biomass. *Photogrammetric Engineering and Remote Sensing*, *46*, 651−656.

Hollinger, D. Y., Aber, J., Dail, B., Davidson, E. A., Goltz, S. M., Hughes, H., et al. (2004). Spatial and temporal variability in forest-atmosphere CO_2 exchange. *Global Change Biology*, *10*, 1689−1706.

Hollinger, D. Y., Goltz, S. M., Davidson, E. A., Lee, J. T., Tu, K., & Valentine, H. T. (1999). Seasonal patterns and environmental control of carbon dioxide and water vapour exchange in an ecotonal boreal forest. *Global Change Biology*, *5*, 891−902.

Huete, A. R., Didan, K., Muira, T., Rodriguez, E. P., Gao, X., & Ferreira, L. G. (2002). Overview of the radiometric and biophysical performance of the MODIS vegetation indices. *Remote Sensing of Environment*, *83*(1-2), 195−213.

Huete, A. R., Liu, H. Q., Batchily, K., & Leeuwen, W. V. (1997). A comparison of vegetation indices over a global set of TM images for EOS-MODIS. *Remote Sensing of Environment*, *59*(3), 440−451.

Hymer, D. C., Moran, M. S., & Keefer, T. O. (2000). Soil water evaluation using a hydrologic model and calibrated sensor network. *Soil Science Society of America Journal*, *64*(1), 319−326.

Jacquemoud, S. (1993). Inversion of the PROSPECT+SAIL canopy reflectance model from AVIRIS equivalent spectra: Theoretical study. *Remote Sensing of Environment*, *44*, 281−292.

Jacquemoud, S., & Baret, F. (1990). PROSPECT, a model of leaf optical properties spectra. *Remote Sensing of Environment*, *34*(2), 75−91.

Jacquemoud, S., Baret, F., Andrieu, B., Danson, F. M., & Jaggard, K. (1995). Extraction of vegetation biophysical parameters by inversion of the

PROSPECT+SAIL models on sugar beet canopy reflectance data. Application to TM and AVIRIS sensors. *Remote Sensing of Environment*, *52*(3), 163−172.

Jacquemoud, S., Ustin, S. L., Verdebout, J., Schmuck, G., Andreoli, G., & Hosgood, B. (1996). Estimating leaf biochemistry using the PROSPECT leaf optical properties model. *Remote Sensing of Environment*, *56*(3), 194−202.

Kleinbaum, D. G., Kupper, L. L., & Muller, K. E. (1988). Comparing Two Straight-line Regression Models. *Applied regression analysis and other multivariable methods* (pp. 95−102). Boston: PWS-Kent 718pp.

Kuusk, A. (1985a). The hot spot effect of a uniform vegetation cover. *Soviet Journal of Remote Sensing*, *3*(4), 645−658.

Kuusk, A. (1995b). A fast, invertible canopy reflectance model. *Remote Sensing of Environment*, *51*(3), 324−350.

Kuusk, A. (1995b). A Markov chain model of canopy reflectance. *Agricultural and Forest Meteorology*, *76*, 221−236.

Kuusk, A. (2001). A two-layer canopy reflectance model. *Journal of Quantitative Spectroscopy & Radiative Transfer*, *71*, 1−9.

Lemeur, R. (1970). Effects of spatial leaf distribution on penetration and interception of direct radiation. *Plant response to climatic factors, Proceedings of the Uppsala Symposium (Ecology and Conservation)* (pp. 349−356). Paris: UNESCO.

Lillesaeter, O. (1982). Spectral reflectance of partly transmitting leaves-Laboratory measurements and mathematical-modeling. *Remote Sensing of Environment*, *12*, 247−254.

Miller, J. R., Hare, E. W., & Wu, J. (1990). Quantitative characterization of the vegetation red edge reflectance: An inverted-Gaussian model. *International Journal of Remote Sensing*, *11*, 1755−1773.

Peñuelas, J., Filella, I., Biel, C., Serrano, L., & Savé, R. (1993). The reflectance at the 950–970 nm region as an indicator of plant water status. *International Journal of Remote Sensing*, *14*, 1887−1905.

Peñuelas, J., Piñol, J., Ogaya, R., & Filella, I. (1997). Estimation of plant water concentration by the reflectance Water Index WI (R900/R970). *International Journal of Remote Sensing*, *18*, 2869−2875.

Riaño, D., Vaughan, P., Zarco-Tejada, E., & Ustin, P. J. (2005). Estimation of fuel moisture content by inversion of radiative transfer models to simulate equivalent water thickness and dry matter content. Analysis at leaf and canopy level. *IEEE Transactions on Geoscience and Remote Sensing*, *43*, 819−826.

Roberts, D. A., Gardner, M., Church, R., Ustin, S. L., Scheer, G., & Green, R. O. (1998). Mapping chaparral in the Santa Monica Mountains using multiple endmember spectral mixture models. *Remote Sensing of Environment*, *65* (3), 267−279.

Roberts, D. A., Green, R. O., & Adams, J. B. (1997). Temporal and spatial patterns in vegetation and atmospheric properties from AVIRIS. *Remote Sensing of Environment*, *62*(3), 223−240.

Roberts, D. A., Ustin, S. L., Ogunjemiyo, S., Greenberg, J., Dobrowski, S. Z., Chen, J., et al. (2004). Spectral and structural measures of northwest forest vegetation at leaf to landscape scale. *Ecosystems*, *7*(5), 545−562.

Rosema, A., Verhoef, W., Noorbergen, H., & Borgesius, J. J. (1992). A new forest light interaction model in support of forest modeling. *Remote Sensing of Environment*, *42*, 23−41.

Rouse, J. W., Hass, R. H., Schell, J. A., & Deering, D. W. (1974). Monitoring vegetation systems in the Great Plains with ERTS. *Proceedings, third Earth Resources Technology Satellite-1 Symposium, Greenbelt, NASA SP-351* (pp. 309–317).

Sellers, P. J. (1985). Canopy reflectance, photosynthesis and transpiration. *International Journal of Remote Sensing*, *6*(8), 1335−1372.

Serrano, L., Ustin, S. L., Roberts, D. A., Gamon, J. A., & Peñuelas, J. (2000). Deriving water content of chaparral vegetation from AVIRIS data. *Remote Sensing of Environment*, *74*(3), 570−581.

Shipley, B., & Vu, T. T. (2001). Dry matter content as a measure of dry matter concentration in plants and their parts. *New Phytologist*, *153*(2), 359−364.

Tucker, C. J. (1980). Remote sensing of leaf water content in the near infrared. *Remote Sensing of Environment*, *10*, 23−32.

Ustin, S. L., Darling, D., Kefauver, S., Greenberg, J., Cheng, Y. -B., & Whiting, M. L. (2004a). Remotely sensed estimates of crop water demand. *S.P.I.E. the international symposium on optical science and technology. 49th annual meeting, Denver, CO, 2–6 August*.

Ustin, S. L., Jacquemoud, S., Zarco-Tejada, P. J., and Asner, G. (2004b). Remote Sensing of Environmental Processes, State of the Science and New Directions. *in Manual of Remote Sensing Vol. 4. Remote Sensing for Natural Resource Management and Environmental Monitoring.* ASPRS. John Wiley and Sons, New York 768p. +cd. (S.L. Ustin, vol. Ed.). ASPRS. John Wiley and Sons, New York, pages 679-730.

Ustin, S. L., Roberts, D. A., Jacquemoud, S., Pinzón, J., Gardner, M., Scheer, G., et al. (1998). Estimating canopy water content of chaparral shrubs using optical methods. *Remote Sensing of Environment*, *65*(3), 280−291.

Verhoef, W. (1984). Light scattering by leaf layers with application to canopy reflectance modeling: the SAIL model. *Remote Sensing of Environment*, *16*, 125−141.

Xiao, X., Boles, S., Liu, J., Zhuang, D., Frolking, S., Li, C., et al. (2005). Mapping paddy rice agriculture in southern China using multi-temporal MODIS images. *Remote Sensing of Environment*, *95*(4), 480−492.

Zarco-Tejada, P. J., Miller, J. R., Morales, A., Berjón, A., & Agûera, J. (2004). Hyperspectral indices and model simulation for chlorophyll estimation in open-canopy tree crops. *Remote Sensing of Environment*, *90*(4), 463−476.

Zarco-Tejada, P. J., Miller, J. R., Noland, T. L., Mohammed, G. H., & Sampson, P. H. (2001). Scaling-up and model inversion methods with narrow-band optical indices for chlorophyll content estimation in closed forest canopies with hyperspectral data. *IEEE Transactions on Geoscience and Remote Sensing*, *39*(7), 1491−1507.

Zarco-Tejada, P. J., Rueda, C. A., & Ustin, S. L. (2003). Water content estimation in vegetation with MODIS reflectance data and model inversion methods. *Remote Sensing of Environment*, *85*(1), 109−124.

Zarco-Tejada, P. J., & Ustin, S. L. (2001). Modeling Canopy Water Content for Carbon Estimates from MODIS data at Land EOS Validation Sites. *IGARRS Meeting, Sydney, Australia, July.*